

# Lattice Boltzmann equation for microscale gas flows of binary mixture

Zhaoli Guo,<sup>1,\*</sup> Pietro Asinari,<sup>2,†</sup> and Chuguang Zheng<sup>1</sup>

<sup>1</sup>*National Laboratory of Coal Combustion,*

*Huazhong University of Science and Technology, Wuhan 430074, P. R. China*

<sup>2</sup>*Department of Energetics, Politecnico di Torino Corso*

*Duca degli Abruzzi 24, Zip Code 10129, Torino, Italy*

(Dated: January 18, 2009)

## Abstract

Modeling and simulating gas flows in/around micro-devices are a challenging task in both science and engineering. In practical applications, a gas is usually a mixture made of different components. In this paper we propose a lattice Boltzmann equation (LBE) model for microscale flows of binary mixture based on a recently developed LBE model for continuum mixtures [P. Asinari and L.-S. Luo, *J. Comput. Phys.* **227**, 3878 (2008)]. A consistent boundary condition for gas-solid interactions is proposed and analyzed. The LBE is validated and compared with theoretical results or other reported data. The results show that the model can serve as a potential method for flows of binary mixture in the microscale.

PACS numbers: 47.61.Cb, 47.61.Fg, 47.45.-n

---

\*Electronic address: [zlguo@mail.hust.edu.cn](mailto:zlguo@mail.hust.edu.cn)

†Electronic address: [pietro.asinari@polito.it](mailto:pietro.asinari@polito.it)

## I. INTRODUCTION

As an efficient mesoscopic method, the lattice Boltzmann equation (LBE) method has gained much success in simulating complex fluid systems such as the hydrodynamics of multi-phase/multi-component fluids, magneto-hydrodynamics, colloidal suspensions, chemical reactions, flows in porous media, etc. [1–3], where the application of other methods may be difficult or impractical. Recently there have been some attempts to apply the LBE method to gaseous microscale flows with non-continuum effects [4–18]. For such flows, the mean-free-path of the gas ( $\lambda$ ) may be comparable to the typical device dimension ( $h$ ), and consequently the flow is far from the thermodynamical equilibrium and the hydrodynamic models such as the classical Navier-Stokes equations for continuum flows are no longer valid. On the other hand, the Boltzmann equation is valid for gas flows with any Knudsen numbers  $\text{Kn} = \lambda/h$  [19], and therefore the LBE, which is a discrete scheme of the Boltzmann equation [20, 21], is believed to have the potential for simulating microscale gas flows.

Although a number of works have shown that the LBE is capable of simulating gas flows with a finite Knudsen number, most of the available models are designed for single-component gases, and much less attentions have been paid to gas mixtures. As far as the authors know, there are very limited works reporting the applications of LBE to micro flows of binary mixtures [22–24]. In Ref. [22], the authors developed a LBE model based on a kinetic model similar to that of Hamel [26], and applied the model to the micro Couette flow to investigate the relationship between the slip coefficients and the species concentration of a binary mixture. It was found that although the tendency of slip coefficient is in good agreement with the kinetic theory and direct simulation Monte Carlo (DSMC) results, the implementation details such as the boundary condition and the specification of relaxation time, were not provided in that paper. Szalmás made a theoretical analysis of a similar LBE model, and proposed a boundary condition for the LBE based on the solution of the half-space Kramers problem [24]. In Ref. [23], Joshi *et al.* studied the Knudsen diffusion of a ternary mixture in a microchannel using a LBE based on the Sirovich model [27]. The Knudsen diffusivity is incorporated into LBE heuristically by matching the LBE results to those of the dusty gas model (DGM). Although the LBE was shown to be able to give good predictions for non-continuum diffusion with this correlation, the method needs further validations.

Although the above mentioned works have shown that the LBE can capture some interesting phenomena in gas mixtures, the LBE models utilized there were all based on the BGK approximation to the Boltzmann equation. As revealed in some recent studies [14–16], the lattice BGK (LBGK) model is exposed to some disadvantages in treating micro flows even for a single gas, while the LBE with multiple relaxation times (MRT-LBE) can overcome these limitations. Therefore, it is expected that a MRT-LBE model would have better properties in modeling micro gas mixtures than LBGK models.

The first MRT-LBE model for binary mixtures was proposed in Ref. [25]. In comparison with other models, this LBE model has two distinct features, (i) the model uses a multi-relaxation-time collision operator where the self-collision and cross-collision among species are both incorporated, (ii) the model has a consistent baroclinic coupling between the species dynamics and the mixture, and satisfies the indifferenciability principle, both of which have not been adequately addressed in previous models. The original version of this LBE model is primarily designed for continuum mixtures. In this work, we will generalize this model to micro flows of binary mixtures. The extension includes two parts. First, a relationship between the relaxation times and the mean-free-paths of the species and mixture is proposed, and second a boundary condition for modeling gas-wall interaction is developed to capture the velocity slip occurring at a wall.

The remainder of this paper is organized as follows. In Sec. II we present a brief introduction of the MRT-LBE model proposed in Ref. [25]. In Sec. III we extend the LBE model for micro flows, where a relationship between the relaxation parameters and the individual and mixture mean-free-paths is derived, and a boundary condition for gas-wall interaction is proposed. Finally, we present some numerical simulations to validate the proposed model in Sec. IV.

## II. MRT-LBE FOR BINNARY MIXTURES

The LBE model with multiple relaxation times for a binary mixture proposed in [25] can be written as

$$f_{\sigma i}(\mathbf{x} + \mathbf{c}_i \delta_t, t + \delta_t) - f_{\sigma i}(\mathbf{x}, t) = \Omega_{\sigma i}(f), \quad (1)$$

for  $i = 0, 1, \dots, q-1$  ( $q$  is the number of discrete velocities) and  $\sigma = a$  and  $b$ , where  $f_{\sigma i}(\mathbf{x}, t)$  is the distribution function for species  $\sigma$  associated with the gas molecules moving with the

discrete velocity  $\mathbf{c}_i$  at position  $\mathbf{x}$  and time  $t$ ,  $\Omega_{\sigma i}(f)$  is the discrete collision operator defined by

$$\Omega_{\sigma i} = - \sum_j (\mathbf{M}^{-1} \mathbf{S} \mathbf{M})_{ij} [f_{\sigma j} - f_{\sigma j}^{(eq)}], \quad (2)$$

where  $\mathbf{M}$  is a  $q \times q$  transform matrix projecting  $f_{\sigma i}$  onto the moment space  $\mathbf{m}_\sigma = \mathbf{M} \mathbf{f}_\sigma$ , where  $\mathbf{f}_\sigma = (f_{\sigma 0}, f_{\sigma 1}, \dots, f_{\sigma, q-1})^\top$ ;  $\mathbf{S} = \text{diag}(\tau_0, \tau_1, \dots, \tau_{q-1})^{-1}$  is a non-negative diagonal matrix with  $\tau_i$  being the relaxation time for the  $i$ -th moment. As  $\tau_i = \tau$ , the MRT model reduces to the BGK model. It is noted that the transform matrix  $\mathbf{M}$  and the relaxation matrix  $\mathbf{S}$  are identical for both species in the original model proposed in [25], which can also be generalized to have different components for different species.

The equilibrium distribution function in Eq. (1) depends on the gas density, velocity, and temperature:

$$f_{\sigma i}^{(eq)} = w_i \rho_\sigma \left[ \alpha_{\sigma i} + \frac{\mathbf{c}_i \cdot \mathbf{u}}{c_s^2} + \frac{(\mathbf{c}_i \cdot \mathbf{u})^2}{2c_s^4} - \frac{u^2}{2c_s^2} \right], \quad (3)$$

where  $\alpha_{\sigma i}$  is a parameter dependent on the molecular mass  $m_\sigma$  and the velocity  $\mathbf{c}_i$ ,  $c_s^2 = RT$  is a model-dependent parameter, where  $R = k_B/m_r$  with  $k_B$  being the Boltzmann constant,  $m_r = \min(m_a, m_b)$  the reference mass, and  $T$  the temperature. For an isothermal system,  $c_s$  is related to the lattice speed  $c = \delta_x/\delta_t$ , where  $\delta_x$  and  $\delta_t$  are the lattice spacing and time step, respectively. The mass density  $\rho$  and velocity  $\mathbf{u}$  of the mixture and those of the species ( $\rho_\sigma$  and  $\mathbf{u}_\sigma$ ) are defined respectively as

$$\rho = \sum_\sigma \sum_i f_{\sigma i}, \quad \rho \mathbf{u} = \sum_\sigma \sum_i \mathbf{c}_i f_{\sigma i}, \quad \rho_\sigma = \sum_i f_{\sigma i}, \quad \rho_\sigma \mathbf{u}_\sigma = \frac{2\tau_d - 1}{2\tau_d} \sum_i \mathbf{c}_i f_{\sigma i} + \frac{\rho_\sigma \mathbf{u}}{2\tau_d}. \quad (4)$$

Obviously,  $\rho = \rho_a + \rho_b$  and  $\rho \mathbf{u} = \rho_a \mathbf{u}_a + \rho_b \mathbf{u}_b$ . The number density of the species and mixture are  $n_\sigma = \rho_\sigma/m_\sigma$  and  $n = n_a + n_b$ , respectively. It is noted that in the original LBE model [25], the  $\sigma$ -species velocity is defined as  $\rho_\sigma \bar{\mathbf{u}}_\sigma = \sum_i \mathbf{c}_i f_{\sigma i}$ . This definition neglects discrete effects of the diffusion force [28]. Actually, this can be seen more clearly from the difference between  $\mathbf{u}_\sigma$  and  $\bar{\mathbf{u}}_\sigma$ :

$$\rho_\sigma (\bar{\mathbf{u}}_\sigma - \mathbf{u}_\sigma) = \frac{\rho_\sigma (\mathbf{u}_\sigma - \mathbf{u})}{2\tau_d - 1} = -\frac{\delta_t}{2} p \mathbf{d}_\sigma,$$

where  $p$  is the total pressure and  $\mathbf{d}_\sigma$  is the diffusion force which will be defined later. This neglect may yield some additional errors in the macroscopical momentum equation as shown in Ref. [28], while the definition in Eq. (4) can avoid such discrete anomalies. Similar

approach was also proposed and discussed in [29], and Ref. [30] proposed a systematic way for defining a consistent velocity by means of variable transformation.

It is noted that the collision term in the LBE (1) includes the effects of both self and mutual collision among gas molecules of identical and different species because the equilibria  $f_{\sigma i}^{(eq)}$  uses the barycentric velocity  $\mathbf{u}$  of the mixture instead of the individual velocity  $\mathbf{u}_\sigma$ . It is easy to verify that the LBE model of (1) also satisfies another important thermodynamic requirement, i.e. the *indifferentiability* principle [31], which means that the LBE (1) for the mixture collapses to the equation for a pure species if two species are identical.

In this work we consider the two-dimensional nine-velocity (D2Q9) LBE model where the discrete velocities  $\mathbf{c}_i$  are defined by  $\mathbf{c}_0 = 0$ ,  $\mathbf{c}_1 = -\mathbf{c}_3 = c(0, 1)$ ,  $\mathbf{c}_2 = -\mathbf{c}_4 = c(1, 0)$ ,  $\mathbf{c}_5 = -\mathbf{c}_7 = c(1, 1)$ , and  $\mathbf{c}_6 = -\mathbf{c}_8 = c(-1, 1)$ ; The weights in the equilibrium distribution functions are  $w_0 = 4/9$ ,  $w_1 = w_2 = w_3 = w_4 = 1/9$ , and  $w_5 = w_6 = w_7 = w_8 = 1/36$ ;  $\alpha_{\sigma i} = s_\sigma = m_r/m_\sigma$  for  $i \neq 0$  and  $\alpha_{\sigma 0} = (9 - 5s_\sigma)/4$ , and  $c_s = \sqrt{RT} = c/\sqrt{3}$ . With out loss of generality, we shall take  $c$  as the velocity unit in the present work. Then, the transform matrix  $\mathbf{M}$  is given by

$$\mathbf{M} = \begin{pmatrix} 1 & 1 & 1 & 1 & 1 & 1 & 1 & 1 & 1 \\ -4 & -1 & -1 & -1 & -1 & 2 & 2 & 2 & 2 \\ 4 & -2 & -2 & -2 & -2 & 1 & 1 & 1 & 1 \\ 0 & 1 & 0 & -1 & 0 & 1 & -1 & -1 & 1 \\ 0 & -2 & 0 & 2 & 0 & 1 & -1 & -1 & 1 \\ 0 & 0 & 1 & 0 & -1 & 1 & 1 & -1 & -1 \\ 0 & 0 & -2 & 0 & 2 & 1 & 1 & -1 & -1 \\ 0 & 1 & -1 & 1 & -1 & 0 & 0 & 0 & 0 \\ 0 & 0 & 0 & 0 & 0 & 1 & -1 & 1 & -1 \end{pmatrix}. \quad (5)$$

The corresponding discrete velocity moments of the distribution functions are

$$\mathbf{m}_\sigma = (\rho_\sigma, e_\sigma, \varepsilon_\sigma, j_{\sigma x}, q_{\sigma x}, j_{\sigma y}, q_{\sigma y}, p_{\sigma xx}, p_{\sigma xy})^\top. \quad (6)$$

These moments have clear physical significance:  $m_{\sigma 0} = \rho_\sigma$  is the density,  $m_{\sigma 1} = e_\sigma$  is related to the total energy,  $m_{\sigma 2} = \varepsilon_\sigma$  is a function of energy square,  $(m_{\sigma 3}, m_{\sigma 5}) = (j_{\sigma x}, j_{\sigma y}) \equiv \sum_i \mathbf{c}_i f_{\sigma i}$  are relevant to the momentum components,  $(m_{\sigma 4}, m_{\sigma 6}) = (q_{\sigma x}, q_{\sigma y})$  depend on the heat flux, and  $m_{\sigma 7} = p_{\sigma xx}$  and  $m_{\sigma 8} = p_{\sigma xy}$  correspond to the diagonal and off-diagonal

components of the stress tensor, respectively. The relaxation matrix corresponding to the nine moments is

$$\mathbf{S} = \text{diag}(\tau_\rho, \tau_e, \tau_\varepsilon, \tau_d, \tau_q, \tau_d, \tau_q, \tau_s, \tau_s)^{-1}, \quad (7)$$

where  $\tau_\rho$  can take any value since  $\rho_\sigma$  is a conserved variable, while the other relaxation times should be chosen according to the transport coefficients.

The hydrodynamic equations for the LBE (1) can be derived using the asymptotic analysis. The mass and momentum equations for each species are as follows,

$$\partial_t \rho_\sigma + \nabla \cdot (\rho_\sigma \mathbf{u}_\sigma) = 0, \quad (8a)$$

$$\partial_t (\rho_\sigma \mathbf{u}_\sigma) + \nabla \cdot (\rho_\sigma \mathbf{u}_\sigma \mathbf{u}) = -\nabla p_\sigma + \nabla \cdot \mathbf{S}^\sigma - \omega_d \rho_\sigma \mathbf{w}_\sigma, \quad (8b)$$

where  $p_\sigma = c_s^2 s_\sigma \rho_\sigma = n_\sigma k_B T$  is the partial pressure,  $\mathbf{w}_\sigma$  is the friction force between species due to velocity difference,

$$\mathbf{w}_\sigma = \mathbf{u}_\sigma - \mathbf{u} = \frac{\rho_\varsigma}{\rho} (\mathbf{u}_\sigma - \mathbf{u}_\varsigma), \quad \varsigma \neq \sigma, \quad (9)$$

and  $\omega_d = 1/(\tau_d - 0.5)\delta_t$ ;  $\mathbf{S}^\sigma$  is a stress-tensor-like term defined by

$$S_{\alpha\beta}^\sigma = \nu [\partial_\alpha (\rho_\sigma u_\beta) + \partial_\beta (\rho_\sigma u_\alpha)] + (\zeta_\sigma - \nu) \nabla \cdot (\rho_\sigma \mathbf{u}) \delta_{\alpha\beta} \quad (10)$$

where  $\nu$  and  $\zeta_\sigma$  are the shear and bulk viscosities, respectively:

$$\nu = c_s^2 \left( \tau_s - \frac{1}{2} \right) \delta_t, \quad \zeta_\sigma = c_s^2 (2 - s_\sigma) \left( \tau_e - \frac{1}{2} \right) \delta_t. \quad (11)$$

Based on the species equations (8), we can obtain the mass and momentum equations for the mixture:

$$\partial_t \rho + \nabla \cdot (\rho \mathbf{u}) = 0, \quad (12a)$$

$$\partial_t (\rho \mathbf{u}) + \mathbf{u} \cdot \nabla \cdot (\rho \mathbf{u}) = -\nabla p + \nabla \cdot \mathbf{S}, \quad (12b)$$

where  $p = p_a + p_b = nk_B T$  is the total pressure, and  $\mathbf{S}$  is the total stress given by

$$S_{\alpha\beta} = \nu [\partial_\alpha (\rho u_\beta) + \partial_\beta (\rho u_\alpha)] + \sum_\sigma (\zeta_\sigma - \nu) \nabla \cdot (\rho_\sigma \mathbf{u}) \delta_{\alpha\beta} \quad (13)$$

For near incompressible flows,

$$S_{\alpha\beta} \approx \mu [\partial_\alpha u_\beta + \partial_\beta u_\alpha]$$

where  $\mu = \rho\nu$  is the dynamic viscosity of the mixture.

In the diffusive scale where  $\partial_t \sim \epsilon^2$ ,  $\nabla \sim \epsilon$ , and  $\mathbf{u} \sim \epsilon$ , the leading order of Eq. (8b) gives that

$$\mathbf{u}_\sigma - \mathbf{u} = -\frac{\nabla p_\sigma}{\omega_d \rho_\sigma} = -D_\sigma \nabla \ln \rho_\sigma, \quad (14)$$

where

$$D_\sigma = \frac{c_s^2 s_\sigma}{\omega_d} = c_s^2 s_\sigma \left( \tau_d - \frac{1}{2} \right) \delta_t \quad (15)$$

is the self-diffusivity. From Eq. (14), we can obtain the velocity difference between the individual species ( $\sigma$  and  $\varsigma$ ),

$$\omega_d(\mathbf{u}_\sigma - \mathbf{u}_\varsigma) = -\frac{\nabla p_\sigma}{\rho_\sigma} + \frac{\nabla p_\varsigma}{\rho_\varsigma} = -\frac{p\rho}{\rho_\sigma \rho_\varsigma} \mathbf{d}_\sigma, \quad (16)$$

where  $\mathbf{d}_\sigma$  is the diffusion force,

$$\mathbf{d}_\sigma = \nabla x_\sigma - (y_\sigma - x_\sigma) \nabla \ln p = -\mathbf{d}_\varsigma, \quad (17)$$

in which  $y_\sigma = \rho_\sigma/\rho$  and  $x_\sigma = n_\sigma/n$ . By definition of mutual diffusivity,

$$x_\sigma x_\varsigma (\mathbf{u}_\sigma - \mathbf{u}_\varsigma) = -D_{\sigma\varsigma} \mathbf{d}_\sigma,$$

we have

$$D_{\sigma\varsigma} = \frac{\rho k_B T}{\omega_d m_\sigma m_\varsigma n} = \frac{m_r \rho}{m_\sigma m_\varsigma n} c_s^2 \left( \tau_d - \frac{1}{2} \right) \delta_t. \quad (18)$$

It can be verified that

$$D_{ab} = \frac{\rho^2}{m_a m_b n^2} \sum_\sigma y_\sigma D_\sigma.$$

Based on Eqs. (11) and (18) the Schmidt number of the mixture can then be expressed as

$$\text{Sc} \equiv \frac{\nu}{D_{\sigma\varsigma}} = \frac{m_a m_b n}{m_r \rho} \frac{\tau_s - 0.5}{\tau_d - 0.5}. \quad (19)$$

It is seen that the relaxation times  $\tau_s$ ,  $\tau_e$ , and  $\tau_d$  are completely determined by the transport coefficients, and the others can be chosen with much freedom in order to enhance numerical stability [32].

### III. EXTENSION OF THE MRT-LBE TO MICRO FLOWS

In order to simulate micro flows of gas mixture using the MRT LBE (1), we must first address two fundamental problems: (i) how to incorporate the Knudsen effect into the LBE, and (ii) how to model the gas-wall interactions through a suitable boundary condition. These two topics will be discussed in order.

### A. Relationship between relaxation times and mean-free-paths

From the Chapman-Enskog analysis of the Boltzmann equation, it is known that the dynamic viscosity and mutual diffusivity of a binary mixture can be expressed as [33]:

$$\mu = \frac{x_a^2 R_a + x_b^2 R_b + x_a x_b R'_{ab}}{x_a^2 R_a / \mu_a + x_b^2 R_b / \mu_b + x_a x_b R_{ab}}, \quad D_{ab} = \frac{3E}{2nm_0}, \quad (20)$$

where  $m_0 = m_a + m_b$ , and

$$R_\sigma = \frac{2}{3} + \frac{m_\sigma}{m_\zeta} A, \quad R'_{ab} = T_a + T_b, \quad R_{ab} = \frac{E}{2\mu_a \mu_b} + \frac{4A}{3EM_a M_b}, \quad (21)$$

with

$$T_\sigma = \frac{E}{2\mu_\sigma} + \frac{2}{3} - A, \quad M_\sigma = \frac{m_\sigma}{m_0}.$$

The parameter  $A$  and  $E$  depend on the inter-molecular potential. For instances, for a binary mixture of hard-sphere molecules [33],

$$A = \frac{2}{5}, \quad E = \sqrt{\frac{2k_B T m_0}{\pi M_a M_b}} \frac{1}{8d_{ab}^2}$$

where  $d_{ab} = (d_a + d_b)/2$  with  $d_\sigma$  being the diameter of molecules of species  $\sigma$ . It is evident from Eq. (20) that the viscosity and diffusivity of the mixture are both complicated functions of the individual viscosities and concentrations.

On the other hand, it is known from the kinetic theory that the mean-free-path  $\lambda_\sigma$  of the single gas  $\sigma$  can be determined from the dynamic viscosity  $\mu_\sigma$  as [19],

$$\lambda_\sigma = \frac{\mu_\sigma}{p_\sigma} \sqrt{\frac{\pi k_B T}{2m_\sigma}}. \quad (22)$$

The above expression can be generalized to a binary mixture (e.g., [34, 35]),

$$\lambda = \frac{\mu}{p} \sqrt{\frac{\pi k_B T}{2m_x}}. \quad (23)$$

where  $m_x = \rho/n = x_a m_a + x_b m_b$ .

For the D2Q9 LBE model described in the above section, the viscosity of the mixture is related to the relaxation times  $\tau_s$ , and therefore we can obtain the following  $\tau_s - \lambda$  relationship,

$$\lambda = \sqrt{\frac{\pi m_x}{2k_B T}} c_s^2 \left( \tau - \frac{1}{2} \right) \delta_t = \sqrt{\frac{\pi m_x}{3m_r}} \left( \tau_s - \frac{1}{2} \right) \delta_t, \quad (24)$$



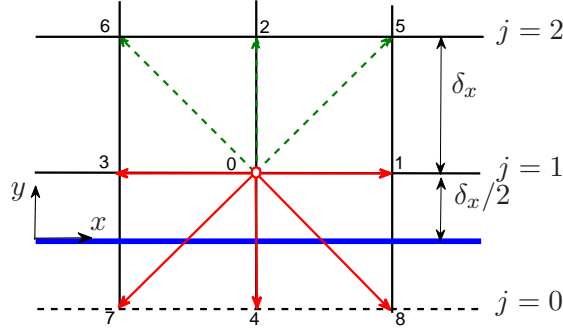


FIG. 1: (Color online) Schematic of the flow geometry and lattice arrangement.

where we have used the fact that  $c_s^2 = k_B T / m_r = 1/3$  for the D2Q9 model. The relaxation time  $\tau_d$  can also be related to the mean-free-path. For instance, for a binary mixture of hard sphere gases, the mean-free-path of each species is

$$\lambda_\sigma = \frac{1}{\sqrt{2}n_i\pi\sigma_i^2}, \quad \sigma = a, b. \quad (25)$$

The mutual diffusivity of the mixture can then be expressed as

$$D_{ab} = \frac{3E}{2nm_0} = \frac{3}{2}\sqrt{\frac{m_0 k_B T}{m_a m_b}} \left[ \frac{1}{\sqrt{x_a \lambda_a}} + \frac{1}{\sqrt{x_b \lambda_b}} \right]^{-2}. \quad (26)$$

Therefore, according to Eq. (18) the relaxation time  $\tau_d$  can be determined from  $D_{ab}$  as

$$\left( \tau_d - \frac{1}{2} \right) \delta_t = \frac{3}{2}\sqrt{\frac{3m_0 m_a m_b}{m_r m_x^2}} \left[ \frac{1}{\sqrt{x_a \lambda_a}} + \frac{1}{\sqrt{x_b \lambda_b}} \right]^{-2}. \quad (27)$$

It should be noted that  $\tau_s$  and  $\tau_d$  can also be recast in terms of the Knudsen numbers of the mixture and/or species since  $\text{Kn}_i = \lambda_i/h$ .

## B. Kinetic boundary condition for the MRT LBE

Suitable boundary conditions must be supplied for the MRT LBE (1) in practical applications. Some schemes, such as the discrete Maxwell's diffuse-reflection (DMDR) scheme and the combined bounce-back/specular-reflection (BSR) scheme, have been proposed for MRT-LBE in the case of single gas [15]. It was shown that for single component flows these two schemes are actually identical in a parametric range where both are applicable, and both contain some discrete effects [15] that should be corrected. In this work we will concentrate on the BSR scheme since its applicable range is wider than the DMDR one.

For simplicity we consider a flat surface as sketched in Fig. 1. The lattice is arranged so that the solid wall locates at  $j = 1/2$ , where  $j$  is the index of the grid line at  $y_j = (j - 0.5)\delta_x$ . After the streaming step,

$$f_{\sigma i}(\mathbf{x} + \mathbf{c}_i \delta_t, t + \delta_t) = \tilde{f}_{\sigma i}(\mathbf{x}, t),$$

where  $\tilde{f}_{\sigma i}(\mathbf{x}, t) = f_{\sigma i}(\mathbf{x}, t) + \Omega_{\sigma i}(\mathbf{x}, t)$  is the post-collision distribution function, we can obtain the new distribution functions at all nodes of  $j > 1$ . But for nodes at  $j = 1$ , only  $f_{\sigma 0}^1$ ,  $f_{\sigma 1}^1$ ,  $f_{\sigma 3}^1$ ,  $f_{\sigma 7}^1$ , and  $f_{\sigma 8}^1$  can be determined in the streaming step, while the remaining distribution functions,  $f_{\sigma 2}^1$ ,  $f_{\sigma 5}^1$ , and  $f_{\sigma 6}^1$ , must be specified according to the kinetic boundary conditions at the wall. For the BSR scheme, these unknown distribution functions are given by

$$\begin{aligned} f_{\sigma 2}^1 &= \tilde{f}_{\sigma 4}^1 + 2r_\sigma \rho_\sigma \mathbf{c}_2 \cdot \mathbf{u}_w / c_s^2, \\ f_{\sigma 5}^1 &= r_\sigma \tilde{f}_{\sigma 7}^1 + (1 - r_\sigma) \tilde{f}_{\sigma 8}^1 + 2r_\sigma \rho_\sigma \mathbf{c}_5 \cdot \mathbf{u}_w / c_s^2, \\ f_{\sigma 6}^1 &= r_\sigma \tilde{f}_{\sigma 8}^1 + (1 - r_\sigma) \tilde{f}_{\sigma 7}^1 + 2r_\sigma \rho_\sigma \mathbf{c}_6 \cdot \mathbf{u}_w / c_s^2, \end{aligned} \quad (28)$$

where  $0 \leq r_\sigma \leq 1$  is the portion of the bounce-back part. Note that  $r_\sigma$  may be different for different species.

Now we analysis the hydrodynamic behavior of the LBE (1) under the boundary condition of (28). The method employed here is similar to that used in previous studies [12, 14]. To simplify the analysis, we consider the half space shear flow over a stationary wall (Kramers' problem, [19]) where the wall located at  $y = 0$  and the gas in the  $y > 0$  region is sheared by imposing a fixed velocity gradient at  $y = \infty$ . The flow is assumed to be unidirectional and satisfy the following condition,

$$\frac{\partial \phi}{\partial t} = 0, \quad \rho_\sigma = \text{const}, \quad v_\sigma = u_{\sigma y} = 0, \quad v = u_y = 0, \quad \frac{\partial \phi}{\partial x} = 0, \quad (29)$$

where  $\phi$  is an arbitrary flow variable. Under such conditions, by expanding the left-hand side of the LBE (1) into a Taylor series in  $\delta_t$  up to second-order, we can obtain that

$$c_{iy} \partial_y f_{\sigma i} + \frac{\delta_t}{2} c_{iy}^2 \partial_y^2 f_{\sigma i} = \Omega'_{\sigma i}(f), \quad (30)$$

where  $\Omega'_\sigma = \mathbf{M}^{-1} \mathbf{S}' \mathbf{M} [f_\sigma - f_\sigma^{(\text{eq})}]$  with  $\mathbf{S}' = \mathbf{S} / \delta_t$ . Multiplying both hand sides of Eq. (30) by the transform matrix  $\mathbf{M}$ , we can get the following equations for the moments:

$$\partial_y p_{\sigma xy} + \frac{\delta_t}{2} \partial_y^2 \left[ \frac{2\rho_\sigma \bar{u}_\sigma}{3} + \frac{q_{\sigma x}}{3} \right] = -\frac{\rho_\sigma (\bar{u}_\sigma - u)}{\tau_d \delta_t}, \quad (31a)$$

$$\partial_y p_{\sigma xy} + \frac{\delta_t}{2} \partial_y^2 \left[ \frac{2\rho_\sigma \bar{u}_\sigma}{3} + \frac{q_{\sigma x}}{3} \right] = -\frac{q_{\sigma x} + \rho_\sigma u}{\tau_q \delta_t}, \quad (31b)$$

$$\partial_y \left[ \frac{2\rho_\sigma \bar{u}_\sigma}{3} + \frac{q_{\sigma x}}{3} \right] + \frac{\delta_t}{2} \partial_y^2 p_{\sigma xy} = -\frac{p_{\sigma xy}}{\tau_s \delta_t}, \quad (31c)$$

where

$$\rho_\sigma \bar{u}_\sigma \equiv j_{\sigma x} = \rho_\sigma u_\sigma + \frac{\rho_\sigma (u_\sigma - u)}{2\tau_d - 1}, \quad \rho u = \sum_\sigma \rho_\sigma u_\sigma = \sum_\sigma \rho_\sigma \bar{u}_\sigma.$$

Equations (31a) and (31b) give that

$$q_{\sigma x} = -\rho_\sigma u + \frac{\tau_q}{\tau_d} \rho_\sigma (\bar{u}_\sigma - u), \quad (32)$$

while Eqs. (31a) and (31c) give that (neglecting terms of  $O(\delta_t^2)$ )

$$\left(1 - \frac{1}{2\tau_s}\right) \partial_y p_{\sigma xy} = -\frac{1}{\tau_d \delta_t} \rho_\sigma (\bar{u}_\sigma - u), \quad (33a)$$

$$\partial_y \left[ \frac{2\rho_\sigma \bar{u}_\sigma}{3} + \frac{q_{\sigma x}}{3} - \frac{1}{2\tau_d} \rho_\sigma (\bar{u}_\sigma - u) \right] = -\frac{1}{\tau_s \delta_t} p_{\sigma xy}, \quad (33b)$$

from which we can obtain

$$\nu \partial_y^2 \left[ \rho_\sigma \bar{u}_\sigma + \frac{\tau_d + \tau_q - 3/2}{\tau_d} \rho_\sigma (\bar{u}_\sigma - u) \right] = \frac{\rho_\sigma (\bar{u}_\sigma - u)}{\tau_d \delta_t}, \quad (34)$$

where  $\nu = \frac{1}{3}(\tau_s - 0.5)\delta_t$ . Taking summation of Eq. (34) over  $\sigma$  leads to

$$\partial_y^2 u = 0, \quad (35)$$

which means that the LBE (1) is actually a second-order scheme for this equation. The solution of Eq. (35) is

$$u = u_s + \gamma y, \quad (36)$$

where  $u_s$  is the slip velocity of the mixture velocity dependent on the boundary condition, and  $\gamma$  is the specified velocity gradient at  $y = \infty$ . Equations (34) and (35) indicate that

$$\nu \left( 2\tau_d + \tau_q - \frac{3}{2} \right) \delta_t \partial_y^2 (\bar{u}_\sigma - u) = \bar{u}_\sigma - u, \quad (37)$$

or

$$\nu \left( 2\tau_d + \tau_q - \frac{3}{2} \right) \delta_t \partial_y^2 (u_\sigma - u) = u_\sigma - u, \quad (38)$$

whose solution is

$$u_\sigma = u + l_\sigma e^{By} + k_\sigma e^{-By}, \quad B = \left[ \nu \left( 2\tau_d + \tau_q - \frac{3}{2} \right) \delta_t \right]^{-1/2} \quad (39)$$

where  $l_\sigma$  and  $k_\sigma$  are two constants depends on the boundary condition of the species velocity. Since  $\partial_y u_\sigma$  is finite as  $y \rightarrow \infty$ ,  $l_\sigma$  must be zero, and thus the velocity of species  $\sigma$  is

$$u_\sigma = u_s + \gamma y + k_\sigma e^{-By}. \quad (40)$$

Because  $\rho u = \rho_\sigma u_\sigma + \rho_\varsigma u_\varsigma$ , the parameter  $k_\sigma$  must satisfy  $\rho_\sigma k_\sigma + \rho_\varsigma k_\varsigma = 0$ . Substituting  $u_\sigma$  and  $u$  into Eq. (33b) we can obtain that

$$p_{\sigma xy} = -\frac{\tau_s \delta_t}{3} \rho_\sigma \left[ \gamma - \left( 2 + \frac{2\tau_q - 1}{2\tau_d - 1} \right) k_\sigma B e^{-By} \right]. \quad (41)$$

In order to determine the slip velocity  $u_s$  and the constant  $k_\sigma$ , we now turn to the boundary condition given by Eq. (28). First, based on the relationship between the distribution functions  $f_\sigma$  and the moments  $\mathbf{m}_\sigma$ , we have

$$F_{56}^\sigma \equiv f_{\sigma 5} - f_{\sigma 6} = \frac{1}{3} j_{\sigma x} + \frac{1}{6} q_{\sigma x} + \frac{1}{2} p_{\sigma xy}, \quad (42)$$

and

$$\tilde{F}_{87}^\sigma \equiv \tilde{f}_{\sigma 8} - \tilde{f}_{\sigma 7} = \frac{1}{3} \tilde{j}_{\sigma x} + \frac{1}{6} \tilde{q}_{\sigma x} - \frac{1}{2} \tilde{p}_{\sigma xy}, \quad (43)$$

where the post-collision moments are given by

$$\tilde{j}_{\sigma x} = j_{\sigma x} - \frac{1}{\tau_d} (j_{\sigma x} - \rho_\sigma u), \quad (44a)$$

$$\tilde{q}_{\sigma x} = q_{\sigma x} - \frac{1}{\tau_q} (q_{\sigma x} + \rho_\sigma u), \quad (44b)$$

$$\tilde{p}_{\sigma xy} = \left( 1 - \frac{1}{\tau_s} \right) p_{\sigma xy}. \quad (44c)$$

With the aids of Eqs. (36), (40), and (41), we can obtain that

$$F_{56}^\sigma(y_1) = \frac{\rho_\sigma}{6} \left[ u_s - (\tau_s - 0.5) \delta_t \gamma + \Lambda_1 k_\sigma e^{-By_1} \gamma \delta_t \right], \quad (45)$$

$$\tilde{F}_{87}^\sigma(y_1) = \frac{\rho_\sigma}{6} \left[ u_s + (\tau_s - 0.5) \delta_t \gamma + \Lambda_2 k_\sigma e^{-By_1} \gamma \delta_t \right], \quad (46)$$

where  $y_1 = \delta_x/2$  is the first grid point, and

$$\Lambda_1 = \frac{4\tau_d + 2\tau_q + (4\tau_d + 2\tau_q - 3) \tau_s \delta_t B}{2\tau_d - 1}, \quad \Lambda_2 = \frac{4\tau_d + 2\tau_q - 6 - (4\tau_d + 2\tau_q - 3) (\tau_s - 1) \delta_t B}{2\tau_d - 1}, \quad (47)$$

It is noted that the BSR scheme given by Eq. (28) gives that

$$F_{56}^\sigma(y_1) = (1 - 2r_\sigma) \tilde{F}_{87}^\sigma(y_1), \quad (48)$$

which can be written explicitly as

$$r_a u_s - \frac{1}{2} [(1 - 2r_a)\Lambda_2 - \Lambda_1] e^{-B\delta_t/2} k = \frac{1}{c_s^2} (1 - r_a) \nu \gamma, \quad (49a)$$

$$r_b u_s + \frac{1}{2} [(1 - 2r_b)\Lambda_2 - \Lambda_1] e^{-B\delta_x/2} k = \frac{1}{c_s^2} (1 - r_b) \nu \gamma, \quad (49b)$$

where  $k$  is an unknown parameter such that  $k_a = y_b k$  and  $k_b = -y_a k$ . The solution of this system is

$$u_s = \left[ \frac{[1 - 2(r_a y_b + r_b y_a)]\Lambda_2 - \Lambda_1}{(r_a y_a + r_b y_b - 2r_a r_b)\Lambda_2 - (r_a y_a + r_b y_b)\Lambda_1} - 1 \right] \frac{\nu \gamma}{c_s^2}, \quad (50a)$$

$$k = \frac{2(r_a - r_b) e^{B\delta_x/2} \nu \gamma}{(r_a y_a + r_b y_b - 2r_a r_b)\Lambda_2 - (r_a y_a + r_b y_b)\Lambda_1} \frac{\nu \gamma}{c_s^2}, \quad (50b)$$

It is interesting to notice that in the special case of  $r_a = r_b = r$ , we have

$$u_s = \frac{(1 - r) \nu \gamma}{r c_s^2}, \quad k = 0, \quad (51)$$

which means that the species and mixture velocities are identical and the profile is linear. Particularly,  $u_s = 0$  as  $r = 1$ , i.e. the pure bounce-back gives the no-slip boundary condition. In general cases, however,  $k$  is nonzero and the velocity of each species will deviate from the linear profile in a region near the wall.

### C. Realization of slip boundary condition

In the slip regime, the effects of gas-wall interaction on the bulk flow can be modeled by a slip boundary condition. The slip velocity at a flat wall can be expressed as [19, 36, 37],

$$u_s = c_m \lambda \gamma, \quad (52)$$

where  $c_m$  is called as velocity slip coefficient (VSC). Based on the solution of the linearized Boltzmann equation for binary mixtures, Ivchenko *et al.* obtained an expression for the VSC [36],

$$c_m = \frac{pM^{1/2}}{\mu} \frac{5\pi}{8} \sum_{\sigma} \left[ (2 - \alpha_{\sigma}) x_{\sigma} b_{\sigma} \left( K_1 + \frac{4b_{\sigma}}{\pi M_{\sigma}^{1/2}} K_2 \right) \right], \quad (53)$$

where  $0 < \alpha_{\sigma} \leq 1$  is the accommodation coefficient of the gas-wall interaction for  $\sigma$  species, and  $M = m_x/m_0$ ;  $b_{\sigma}$  is related to the intermolecular potential of the gases [33, 38],

$$b_{\sigma} = \frac{x_{\sigma} R_{\sigma} + x_{\zeta} T_{\zeta}}{p[x_a^2 R_a / \mu_a + x_b^2 R_b / \mu_b + x_a x_b R_{ab}]}, \quad (54)$$

where the notations can be found in Eq. (21), and  $K_1$  and  $K_2$  are given by

$$K_1 = \frac{\sum_{\sigma} (2 - \alpha_{\sigma}) x_{\sigma} b_{\sigma}}{\sum_{\sigma} \alpha_{\sigma} x_{\sigma} M_{\sigma}^{1/2}} K_2, \quad K_2 = \frac{1}{4(x_a b_a + x_b b_b)} = \frac{p}{4\mu}. \quad (55)$$

It is clear that the VSC  $c_m$  is a function of the species concentration, viscosities, intermolecular potentials, and gas-wall interactions.

Comparing Eq. (53) with Eq. (50a), we can see that in order to realized the velocity boundary condition (52) in the MRT-LBE (1), the control parameter  $r_{\sigma}$  in the BSR scheme must be chosen such that

$$\left[ \frac{[1 - 2(r_a y_b + r_b y_a)] \Lambda_2 - \Lambda_1}{(r_a y_a + r_b y_b - 2r_a r_b) \Lambda_2 - (r_a y_a + r_b y_b) \Lambda_1} - 1 \right] \frac{\nu}{c_s^2} = c_m \lambda. \quad (56)$$

There are many choices for  $r_{\sigma}$  satisfying this condition, and the simplest one is to take  $r_a = r_b = r$ ; In this case, we can obtain from the above condition that  $r$  should be chosen as

$$r = \left[ 1 + \frac{c_m}{3} \sqrt{\frac{\pi m_x}{2k_B T}} \right]^{-1} = \left[ 1 + c_m \sqrt{\frac{\pi m_x}{6m_r}} \right]^{-1}, \quad (57)$$

where we have made use of  $k_B T / m_r = 1/3$  for the D2Q9 model. In the limiting case of a single gas ( $m_a = m_b$ ), the above result is consistent with the result obtained in a previous study [15]. It is noted that other choices of  $r_a$  and  $r_b$  satisfying Eq. (56) are also possible. For example, it is shown that in the case of a single gas  $r_{\sigma}$  is related to the physical accommodation coefficient  $\alpha_{\sigma}$  [14, 15], i.e.

$$\frac{1 - r_{\sigma}}{r_{\sigma}} = \chi \frac{2 - \alpha_{\sigma}}{\alpha_{\sigma}},$$

where  $\chi$  is a constant dependent on the LBE model. Therefore, we can provide the following supplement constraint for Eq. (56):

$$\frac{r_a}{r_b} = \frac{\alpha_a \alpha_b + \chi(2 - \alpha_b)}{\alpha_b \alpha_a + \chi(2 - \alpha_a)}.$$

This constraints ensures that  $r_a \neq \alpha_b$  if  $\alpha_a \neq \alpha_b$ , which is more reasonable. However,  $r_a$  and  $r_b$  would be much complicated in this case. Since different choices of  $r_a$  and  $r_b$  influence the species slip only but have no effects on the mixture slip, in this work we shall use the simplest formulation, i.e. Eq. (57).

#### IV. NUMERICAL RESULTS

We first validate the analytical results presented in the above section. The MRT-LBE (1) is applied to the Kramers problem of a binary mixture with different molecular mass

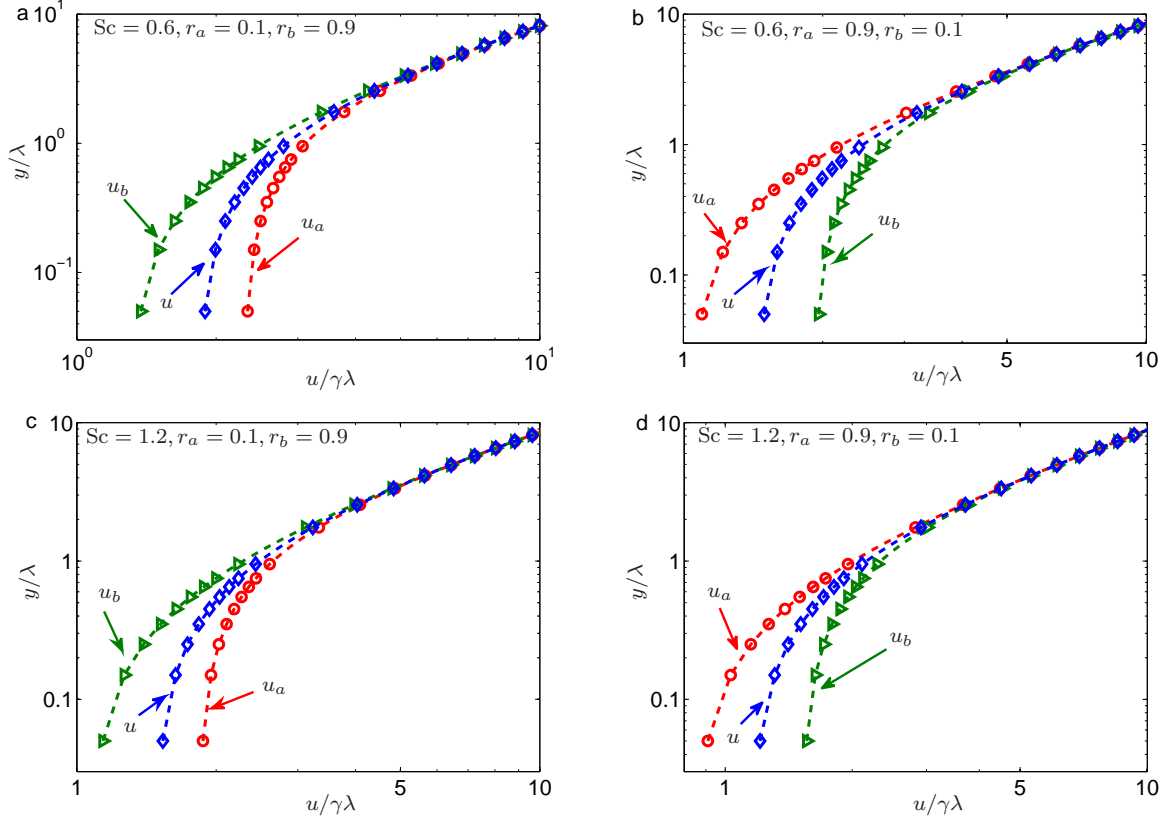


FIG. 2: (Color online) Velocity distributions of each species and mixture. Dashed lines: analytical results given by Eq. (40); symbols: MRT-LBE results.

ratios and concentrations. The mean-free-path of the mixture is set to be the length unit ( $\lambda = 1.0$ ), and the outer boundary is put at  $y = 10\lambda$  where nonslip boundary condition is applied. The relaxation time  $\tau_s$  is determined from  $\lambda$  according to Eq. (24),  $\tau_d$  is then chosen as  $\tau_d = 0.5 + (m_a m_b / m_r m_x \text{Sc})(\tau_s - 0.5)$ , and  $\tau_q$  is set to be identical to  $\tau_d$ ; the other relaxation times are chosen as follows:  $\tau_\rho = 1.0$ ,  $\tau_\epsilon = 1.1$ , and  $\tau_\varepsilon = 1.2$ . It is found in our simulations that the choice of the last three relaxation times has little effects on the numerical results. The simulations are carried out on a mesh of size  $N_x \times N_y = 4 \times 100$ , which means there are about 10 grid points in the Knudsen layer whose size is of order  $\lambda$ . Periodic boundary conditions are applied to the two boundaries at  $x = 0$  and  $x = 4$ , while the BSR scheme is applied to the solid wall with different values of  $r_a$  and  $r_b$ . It is assumed that  $m_a \leq m_b$  so that  $m_r = m_a$  in all of our simulations.

The velocity distributions of the species and mixture predicted by the MRT-LBE with different parameters are measured and compared with the theoretical results given by Eq.

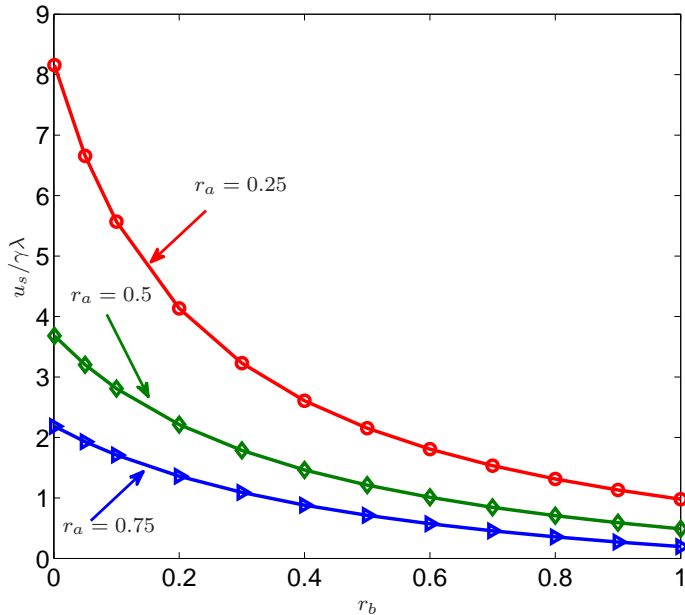


FIG. 3: (Color online) Slip length as a function of  $r_b$  with  $n_a = 0.7$ ,  $n_b = 0.3$ ,  $m_a = 1$ ,  $m_b = 2$ ,  $Sc = 0.8$ . Solid lines: analytical results given by Eq. (50a); symbols: MRT-LBE results.

(40), where  $u_s$  and  $k_\sigma$  are determined by Eq. (50). The molecular masses are set to be  $m_a = 1$  and  $m_b = 2$ , respectively, and the number density is assumed to be  $n_a = 0.7$  and  $n_b = 0.3$ . Figure (2) shows the result with  $Sc = 0.6$  and  $1.2$  at different values of  $r_a$  and  $r_b$ . It is clearly seen from these figures that the numerical results are in excellent with the theoretical ones. Results with other parameters are also obtained (not shown here), and excellent agreement is again observed. The dependence of slip velocity of the mixture,  $u_s$ , on the control parameters  $r_a$  and  $r_b$  in the BSR boundary scheme are also measured. In Fig. (3) the slip length predicted by the LBE are presented together with the theoretical result given by Eq. (40). Again, excellent agreement between the numerical and theoretical results are demonstrated.

The LBE model together with the BSR boundary condition is also applied to the Kramers problem of several binary mixtures composed of practical gases (Ar, CO<sub>2</sub>, H<sub>2</sub>, He, and N<sub>2</sub>). The gases are all modeled as hard-sphere molecules. At standard temperature and pressure, the diameters of Ar, CO<sub>2</sub>, H<sub>2</sub>, He, and N<sub>2</sub> are 3.659, 4.643, 2.745, 2.193, and 3.784 in unit of  $rA$ , respectively, and the molecular masses of these gases are 39.944, 44.011, 2.016, 4.003, and 28.013, respectively [33]. In the simulations, we take the properties of species  $a$  as



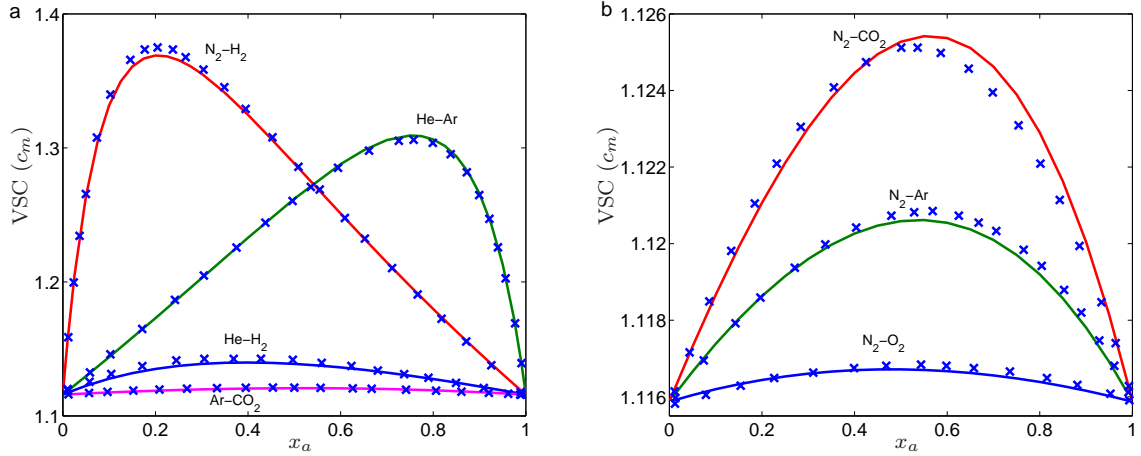


FIG. 4: (Color online) Velocity slip coefficient as a function of concentration of species  $a$  when  $\alpha_a = \alpha_b = 1.0$ . Solid lines are LBE results and symbols ( $\times$ ) are results of linearized Boltzmann equation (Ref. [36])

reference units, i.e.  $m_a = 1$ ,  $n_a = 1$ , and  $d_a = 1$ , and the corresponding properties of species  $b$  are obtained according to the ratios of physical values. With these parameters, the viscosities and mean-free-paths of species and mixtures, and the mutual diffusivity, can be obtained as described in Sec. III. The relaxation times  $\tau_s$  and  $\tau_d$  can then be determined from Eqs. (24) and (27), respectively. The control parameters  $r_a$  and  $r_b$  in the BSR scheme are set to be identical, i.e.  $r_a = r_b = r$  where  $r$  is specified according to Eq. (57), with  $c_m$  given by Eq. (53).

In Fig. 4, the simulated velocity slip coefficients of several binary mixtures are shown as a function of the mole fraction of species  $a$  when the accommodation coefficients of both species are taken to be  $\alpha_a = \alpha_b = 1$ . The results are also compared with those of the linearized Boltzmann equation presented in Ref. [36] where the Lennard-Jones potential is used to model the gases. It is clearly observed that in each case the simulated VSC is in good agreement with the results of the Boltzmann equation, and the nonlinear dependence on the mole concentration is clearly shown. The discrepancies between the LBE predictions and the data in Ref. [36] are due to the different treatments of the intermolecular interactions in the two methods: in the present work, hard-sphere potential is used to model the interaction, while the Lennard-Jones potential is used in Ref. [36]. Despite of these discrepancies, the overall agreement between the results of these two methods is rather good.

## V. SUMMARY

In the present work we have developed a LBE model for microscale flows of binary gas mixtures. The model utilizes a collision operator with multiple relaxation times so that it has good numerical stability and can be applied to mixtures with tunable Schmidt number. A kinetic boundary condition (BSR scheme) that combines the bounce-back and specular-reflection schemes are proposed to model the gas-wall interactions. The scheme was analyzed based on the Kramers problem. It is shown that the velocity of the mixture is a linear function of the distance to the wall, while the species velocities are nonlinear in a region near the wall, each of which decreases or increases exponentially to the mixture velocity. It is also shown that the slip behavior of a binary mixture is influenced by the relaxation times, the Schmidt number, the control parameters in the BSR scheme, and the compositions of the species. A strategy for realizing a slip boundary condition using the BSR scheme was also proposed.

Some numerical simulations were carried out to validate the theoretical results of the proposed LBE and boundary condition. It is shown that the numerical results are in excellent agreement with the analytical results. The LBE is also applied to slip flows of several practical binary mixtures. The simulated VSCs as a function of species concentration is compared with those of linearized Boltzmann equation, and good agreement is observed. In the present work we have concentrated on velocity slip of binary mixtures. Slip behaviors due to concentration and/or temperature gradients will be investigated in future works.

### Acknowledgments

Z.L. Guo is supported by the National Natural Science Foundation of China (No. 50606012 and 50721005) and Program for NCET in University (NCET-07-0323). P. Asinari was supported by the “Program of Introducing Talents of Discipline to Universities of China (B06019)” for his stay at Huazhong University of Science and Technology, during which part of this work was done.

---

[1] S. Chen and G. D. Doolen, *Ann. Rev. Fluid Mech.* **30**, 329 (1998).

- [2] D. Yu, R. Mei, L.-S. Luo, and W. Shyy, *Prog. Aero. Sci.* **39**, 329 (2003).
- [3] S. Succi. *The lattice Boltzmann equation for fluid dynamics and beyond* (Oxford University Press, New York, 2001).
- [4] X. Nie, G. D. Doolen, and S. Chen, *J. Stat. Phys.* **107**, 279 (2002).
- [5] C. Y. Lim, C. Shu, X. D. Niu, *et al.*, *Phys. Fluids* **14** 2299 (2002).
- [6] X. Niu, C. Shu, Y. T. Chew, *EPL* **67**, 600 (2004).
- [7] T. Lee and C. L. Lin, *Phys. Rev. E*, **71**, 046706 (2005).
- [8] M. Sbragaglia and S. Succi, *Phys. Fluids* **17**, 093602 (2005).
- [9] Y. Zhang, R. Qin, and D. R. Emerson, *Phys. Rev. E* **71**, 047702 (2005).
- [10] Z. L. Guo, T. S. Zhao, and Y. Shi, *J. Appl. Phys.* **99**, 074903 (2006).
- [11] Y. H. Zhang, X. J. Gu, R. W. Barber, and D. R. Emerson, *Phys. Rev. E* **74**, 046704 (2006); *Europhys. Lett.* **77**, 30003 (2007).
- [12] S. Ansumali, I. V. Karlin, S. Arcidiacono, *et. al*, *Phys. Rev. Lett* **98**, 124502 (2007).
- [13] Z. L. Guo, B. C. Shi, T. S. Zhao, and Z. G. Zheng, 2007, *Phys. Rev. E* **76**, 056704 (2007).
- [14] Z. L. Guo, Z. G. Zheng, and B. C. Shi, *Phys. Rev. E* **77**, 036707 (2008).
- [15] Z. L. Guo and C. G. Zheng, *Int. J. Comput. Fluid Dyna.* **22** 465 (2008).
- [16] F. Verhaeghe, L.-S. Luo, and B. Blanpain, *J. Comput. Phys.* (unpublished).
- [17] Z. H. Chai, Z. L. Guo, L. Zheng, and B. C. Shi, *J. Appl. Phys.* **104**, 014902 (2008).
- [18] L. Zheng, Z. L. Guo, and B. C. Shi, *EPL* **82** 44002 (2008).
- [19] C. Cercignani, *Mathematical Methods in Kinetic Theory* (Plenum, New York, 1990).
- [20] X. He and L.-S. Luo, *Phys. Rev. E* **55**, R6333 (1997); **56**, 6811 (1997).
- [21] X. Shan and X. He, *Phys. Rev. Lett.* **80**, 65 (1998).
- [22] S. Arcidiacono, I. V. Karlin, J. Mantzaras, and C. E. Frouzakis, *Phys. Rev. E* **76**, 046703 (2007).
- [23] A. S. Joshi, A. A. Peracchio, K. N. Grew, and W. K. S. Chiu, *J. Phys. D: Appl. Phys.* **40**, 7593 (2007).
- [24] L. Szalmás, <http://arxiv.org/abs/0806.1934>
- [25] P. Asinari and L.-S. Luo, *J. Comput. Phys.* **227**, 3878 (2008).
- [26] B. B. Hamel, *Phys. Fluids* **8**, 418 (1965).
- [27] L. Sirovich, *Phys. Fluids* **5**, 908 (1962).
- [28] Z. L. Guo, C. G. Zheng, and B. C. Shi, *Phys. Rev. E* **65**, 046308 (2002).

- [29] P. Asinari, Phys. Rev. E **73**, 056705 (2006).
- [30] P. Asinari, Phys. Rev. E **77**, 056706 (2008).
- [31] P. Andries, K. Aoki, B. Perthame, J. Stat. Phys. **106**, 993 (2002).
- [32] P. Lallemand and L.-S. Luo, Phys. Rev. E **61**, 6546 (2000).
- [33] S. Chapman and T. G. Cowling, *The Mathematical Theory of Non-Uniform Gases* 3rd ed. (Cambridge University Press, Cambridge, 1970).
- [34] Y. I. Yalamov, A. A. Yushkanov and S. A. Savkov, J. Engng. Phys. Thermophy. **66**, 421 (1994).
- [35] F. Sharipov and D. Kalempa, J. Vac. Sci. Technol. A **20**, 814 (2002).
- [36] I. N. Ivchenko, S. K. Loyalka, and R. V. Tompson, J. Vac. Sci. Technol. A **15**, 2375 (1997).
- [37] I. N. Ivchenko, S. K. Loyalka, and R. V. Tompson, Z. Angew. Math. Phys **53**, 58 (2002).
- [38] S. K. Loyalka, Phys. Fluids **14**, 2599 (1971).